Thermal relaxation of the electric conductivity in amorphous silicon-germanium alloys

Jeffrey Zhaohuai Liu, V. Chu, D. S. Shen,* D. Slobodin,† and S. Wagner
Department of Electrical Engineering, Princeton University, Princeton, New Jersey 08544
(Received 15 May 1989)

We report the first observation of the effect of thermal annealing and quenching on the dark and photoelectric conductivities in hydrogenated and fluorinated amorphous silicon-germanium alloys (*a*-Si,Ge:H,F). A reversible glasslike transition of the dark and photoconductivities was observed and was used to estimate a freeze-in temperature of about 140 °C for alloys with optical gaps of about 1.4 eV. This observation suggests thermal-equilibrium processes of defect states in the alloys. The possible implication to solar-cell performance is discussed.

Metastability has been an important problem in the fundamental understanding of amorphous semiconductors and their applications.[1] For a long time, the metastability in hydrogenated amorphous silicon (*a*-Si:H) and silicon-germanium alloys (*a*-Si,Ge:H,F) had been related only to the optical generation of defects and the thermal annealing of these defects.[2] Recently, it was found that defects in *a*-Si:H can also be induced thermally. Thus, a sample at different temperatures contains different numbers of defects, provided that it is kept at each temperature long enough to establish each thermally stable state—a thermal-equilibration process.[3] This discovery has led to much research interest.[4] A related issue is the relaxation time which is required for the thermally stable state to be established. As the temperature decreases from high temperature, the relaxation time increases and the number of defects and related physical quantities will exhibit a glasslike transition. Indeed, a glasslike transition was recently reported in boron- and phosphorus-doped *a*-Si:H using the sweep-out technique, which presumably measures the density of occupied band-tail states in doped *a*-Si:H.[5]

An important class of materials closely related to *a*-Si:H is *a*-Si,Ge:H,F.[1] Because of the large initial number of defects in even the best alloys available to date, extreme care must be exercised to reduce experimental error to observe a clear glasslike transition behavior. In this paper, we report the first observation of the glasslike transition behavior of dark and photoconductivities in *a*-Si,Ge:H,F. This observation suggests the thermal equilibration of the defect states in the alloys. The freeze-in temperature is estimated to be 140 °C for the alloys with optical band gaps of about 1.4 eV.

The samples used in this study are labeled *A* and *B*, corresponding to our laboratory labels *GP*47 and *GP*46, respectively. They were grown from dc glow discharges in SiF_4, GeF_4, and H_2.[6] The deposition conditions and some of the initial properties are given in Tables I and II, respectively.

In the fast-cooling (FC) experiments, the samples were first annealed in nitrogen at temperature T_a for 10 min and then cooled to room temperature at an average rate of about 20 °C/sec. This cooling rate was obtained by dropping the samples onto a room-temperature glass dish in air, followed by flushing the samples with room-temperature nitrogen gas. In the slow-cooling (SC) experiments, the samples were annealed in nitrogen at annealing temperature T_a for 10 min, and then cooled in nitrogen at a constant rate of 5 °C/min. After the sample was annealed at T_a and cooled (FC or SC) to room temperature, dark and photoconductivities were measured. The annealing-cooling-measurement cycles were repeated with different T_a and/or cooling rate (FC or SC) to monitor the effect of the thermal treatments.

Dark and photoconductivities were used to monitor the thermal processes. Conductivities were measured with parallel Cr electrodes evaporated on top of the films. The gap between the electrodes was 0.65 cm long and 0.1 cm wide. Applied voltages were within the Ohmic region at all stages of the thermal treatment and were 100 and 50 V for samples *A* and *B*, respectively. For the photoconductivity (σ_{ph}) measurement, a tungsten lamp was used with an ~50-nm-wide bandpass filter to produce nearly uniform illumination in the samples. Here, the photoconductivity is defined as the conductivity under illumination minus the dark conductivity. To prevent light-induced defects, the light intensity for photoconductivity was adjusted so that only 3–10 times the dark conductivity was obtained. The generation rates were

TABLE I. Deposition conditions for the samples. T_s is the nominal substrate temperature.

	Gas-flow rate								Deposition	
Sample	SiF_4 (sccm)	GeF_4 (sccm)	H_2 (sccm)	T_s (°C)	Voltage (V)	Current (mA)	Power density (W/cm^2)	Pressure (Torr)	rate (Å/sec)	Thickness (μm)
A	28	0.4	7	280	530	50	0.76	0.31	1.9	1.7
B	28	0.7	7	260	530	50	0.71	0.31	1.8	4.2

 ©1989 The American Physical Society

TABLE II. Some initial properties of the samples. E_g is the Tauc gap, E_u the inverse slope of the Urbach tail in the optical spectrum acquired with constant photocurrent method (CPM), N_s the defect concentration inferred from the integrated excess subgap absorption $[1.9\times10^{16}\int(\Delta\alpha)_{\rm CPM}dE]$, σ_d the dark conductivity, $\sigma_{\rm ph}$ the photoconductivity at a generation rate of about 1×10^{20} cm^{-3}sec^{-1}, and γ the photoconductivity-generation-rate exponent ($\sigma_{\rm ph}\propto G^{\gamma}$).

Sample	E_g (eV)	E_u (meV)	N_s (cm^{-3})	σ_d (S/cm)	$\sigma_{\rm ph}$ (S/cm)	γ
A	1.47	62	1×10^{16}	8.7×10^{-9}	4.3×10^{-5}	0.76
B	1.33	60	7×10^{16}	1.4×10^{-8}	1.8×10^{-5}	0.71

8×10^{16} and 6×10^{17} cm^{-3}sec^{-1} for samples *A* and *B*, respectively.

Shown in the main figure of Fig. 1 is the dark conductivity σ_d versus measurement temperature T_m after slow cooling and fast cooling from different annealing temperatures T_a, for sample *A*. Each set of data of σ_d versus T_m was obtained stepwise in the course of heating the sample from room temperature to about 130 °C at an average heating rate 4±1 °C/min. The numerical labels 1–6 show the sequence of thermal treatments and measurements. The insert to Fig. 1 shows the variation of the activation energy E_a of the dark conductivity with annealing temperature T_a. Thus, fast cooling from a high T_a reduces σ_d (and $\sigma_{\rm ph}$, see below) and increases E_a. The coincidence of data sets 1 and 6 in Fig. 1 shows that the effect is reversible. The effect on conductivity is similar to the Staebler-Wronski effect in *a*-Si:H (Ref. 7) and to the quench-in of dark conductivity in undoped *a*-Si:H.[8]

In Fig. 2(a) we show for sample *A* the normalized resistivity ($\rho_d\equiv1/\sigma_d$ and $\rho_{\rm ph}\equiv1/\sigma_{\rm ph}$) measured at $T_m=27.5$°C as a function of the annealing temperature T_a in the fast-cooling and slow-cooling experiments. The FC and SC data were taken in separate experiments. In each (FC or SC) experiment, the annealing (at T_a) -cooling (FC or SC) -measurement (at T_m) cycles were repeat-

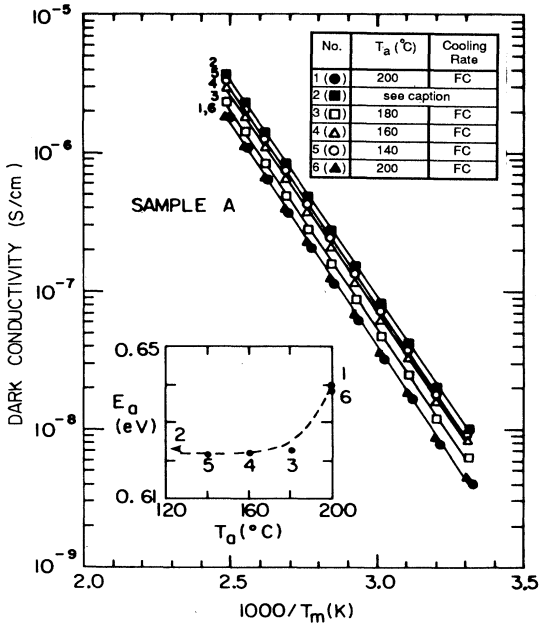

FIG. 1. Main figure: dark conductivity vs measurement temperature T_m after thermal treatment. The solid lines are the least-squares regression fits to the data. Inset: E_a is the activation energy of the dark conductivity; the dashed curve is a guide to eye. The annealing temperature T_a (in °C) and cooling rate are (1) 200, fast cooling (FC); (3) 180, FC; (4) 160, FC; (5) 140, FC; (6) 200, FC. Data set 2 was taken after the sample had gone through the annealing (at T_a) and slow-cooling (5 °C/min from T_a to room temperature) cycles with T_a in the sequence of 200, 180, 160, 140, 120, 100, and 80 °C. The data were taken from sample *A*.

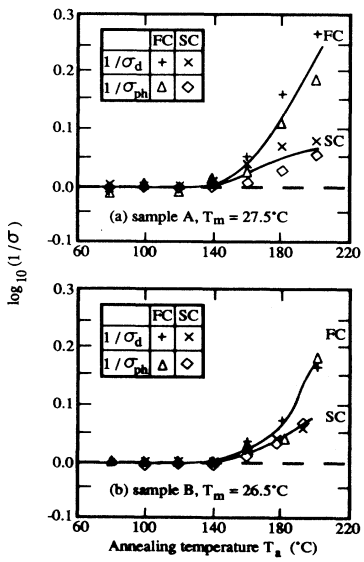

FIG. 2. $\log_{10}(\rho_d/\rho_{d,\rm norm})$ and $\log_{10}(\rho_{\rm ph}/\rho_{\rm ph,norm})$ measured at temperature T_m as a function of annealing temperature T_a in the fast-cooling (FC) and slow-cooling (SC) experiments. $\rho_d\equiv1/\sigma_d$ is the dark resistivity and $\rho_{\rm ph}\equiv1/\sigma_{\rm ph}$ the resistivity under the illumination. The normalization factors $\rho_{d,\rm norm}$ and $\rho_{\rm ph,norm}$ are the saturation values of the respective resistivity in each sequence of the thermal treatments. In (a), $\rho_{d,\rm norm}=1.15\times10^{8}$ Ω cm and $\rho_{\rm ph,norm}=4.93\times10^{7}$ Ω cm for FC data; $\rho_{d,\rm norm}=1.06\times10^{8}$ Ω cm and $\rho_{\rm ph,norm}=5.83\times10^{7}$ Ω cm for SC data. In (b), $\rho_{d,\rm norm}=6.94\times10^{7}$ Ω cm and $\rho_{\rm ph,norm}=1.61\times10^{7}$ Ω cm for FC data; $\rho_{d,\rm norm}=6.76\times10^{7}$ Ω cm and $\rho_{\rm ph,norm}=1.50\times10^{7}$ Ω cm for SC data. The curves are guides to the eye.

ed with different annealing temperature T_a. The cycles started with $T_a = 200\,^{\circ}\mathrm{C}$, T_a was reduced stepwise for each subsequent cycle. The behavior of σ_d and σ_{ph} is similar. We first analyze the FC curve. At high T_a, thermal equilibrium is reached within the annealing time. The cooling rate is larger than the relaxation rate of the system. Therefore, the fast cooling freezes in the configuration of the system at T_a. Fast cooling from lower T_a yields higher σ_d and σ_{ph}. At low T_a, the FC curve saturates. This is due to the increase of the relaxation time as temperature decreases. When the relaxation time is longer than the annealing time (which is 10 min in this study), the system retains its configuration of the lowest T_a at which thermal equilibrium was reached. When the system is cooled slowly from T_a, the SC curve is followed. As in the case of FC, thermal equilibrium is reached during the annealing at high T_a. But now the cooling rate is smaller than the relaxation rate of the system at high temperature so that the system can follow the cooling. As the sample is cooled, the relaxation time increases and at low enough temperature the system cannot follow the cooling. Therefore, with slow cooling from high T_a, the configuration of the system freezes in at temperatures lower than T_a. This causes the SC curve to lie lower than the FC curve at high T_a. Again, the effect saturates when T_a is low. The effect is shown for sample B in Fig. 2(b).

Therefore, Fig. 2 shows the following features. (1) The relaxation rate is temperature dependent. (2) The relaxation time at high T_a (above about 160 °C) is shorter than the annealing time (10 min). (3) The relaxation time at high T_a is so short that the system can follow the slow cooling (5 °C/min), but it is long enough so that the annealed states can be frozen in by fast cooling (about 20 °C/sec). (4) The relaxation time at low T_a is longer than the annealing time (10 min). The data of Fig. 2 are reminiscent of a glass transition, and suggest the existence of a thermal equilibrium process at high T_a. If we assume that the change of the dark and photoconductivities corresponds to change of defect states in the materials, as is the case in the optical generation of defects, then our observations indicate thermal equilibration of the defect states in the materials. The freeze-in temperature T_f is defined as the temperature where the fast- and slow-cooling curves merge. From Fig. 2, we estimated a T_f of about 140 °C for both samples.

Similar thermal processes of various physical quantities have been observed in a-Si:H (Refs. 3, 5, and 9) and the higher-gap alloys (a-Si,C:H).[10] The freeze-in temperature T_f depends on the annealing time t_a. But it is not very sensitive to t_a, because the relaxation time of the system increases very fast as the temperature decreases. Therefore, it is meaningful to compare the freeze-in temperature T_f reported from different laboratories. T_f for a-Si:H is $\sim 200\,^{\circ}\mathrm{C}$ ($t_a = 30$ min).[3,9,10] As a-Si:H is alloyed with either carbon or germanium, or doped, T_f decreases. In a-Si,C:H, T_f is $\sim 150\,^{\circ}\mathrm{C}$ ($t_a = 30$ min) when the carbon concentration is $\sim 18\%$.[10] In a-Si,Ge:H,F, the present data indicate that T_f is $\sim 140\,^{\circ}\mathrm{C}$ ($t_a = 10$ min) when the germanium concentration[11] is $\sim 35\%$. T_f is $\sim 130\,^{\circ}\mathrm{C}$ ($t_a = 10$ min) for n-type-doped a-Si:H, and $\sim 80\,^{\circ}\mathrm{C}$ ($t_a = 10$ min) for p-type-doped a-Si:H.[5] The decrease of T_f reflects a decrease of the relaxation time of the system, i.e., an increase of the strength of interaction and/or of the number of channels of interaction in the system. Because alloying and doping introduce defects, one may relate the decrease of the freeze-in temperature T_f upon alloying and doping to the increase of the total number of defects. The defects may play a role of interaction "channels" in the thermal equilibration. It is also possible to have different mechanisms of defect equilibration for different kinds of materials (a-Si:H, a-Si,C:H, a-Si,Ge:H,F, and doped a-Si:H). In doped a-Si:H, the defect equilibration was explained by using the defect compensation model of doping plus the assumption of a temperature-dependent relaxation rate for the structure.[5] In a-Si,Ge:H,F, as the germanium concentration increases, the band gap E_g and the energy difference between the peak of $D^{0/-}$ defect-band and the valence-band edge, E_{DV}, decrease.[12] If one speculates that E_{DV} is the activation energy of the relaxation rate for the defects, then as the germanium concentration increases, the relaxation rate will increase and the freeze-in temperature will decrease. As reported here, the freeze-in temperature decreases from about 200 °C for a-Si:H to about 140 °C for a-Si,Ge:H,F with about 35% germanium. This proposed dependence of the freeze-in temperature on the germanium concentration is to be tested in an extended range of germanium concentrations. This proposal is interesting for solar-cell application because it implies that the operation temperature of solar cells made from low-gap amorphous silicon germanium alloys may be close to the freeze-in temperature and thus there may be no light-induced degradation.

In summary, we have observed the effect of thermal annealing and quenching on σ_d and σ_{ph} in two a-Si,Ge:H,F alloys with band gaps 1.47 and 1.38 eV. The annealed and then fast-cooled state has lower dark and photoconductivities than the annealed and then slowly cooled state. The thermal effect is reversible. The conductivity shows a glasslike transition behavior as the annealing temperature changes. These observations suggest thermal equilibration of defect states in the alloys. From the glasslike transition behavior of the conductivity, we have estimated the freeze-in temperatures to be about 140 °C for both samples.

We are grateful to S. Tanaka and E. Boyd for their help in the experiments. This work is supported by the Electric Power Research Institute under Contract No. RP2824-2.

*Present address: Glasstech Solar, Inc., 12441 West 49th Ave., Wheatridge, CO 80033.

†Present address: Greyhawk Systems, 1557 Centre Pointe Dr., Milpitas, CA 95035.

[1]See, for example, *Stability of Amorphous Silicon Alloy Materials and Devices,* Proceedings of an International Conference on Stability of Amorphous Silicon Alloy Materials and Devices, AIP Conf. Proc. No. 157, edited by B. L. Stafford and E. Sabisky (AIP, New York, 1987).

[2]See, for example, *Optical Effects in Amorphous Semiconductors (Snowbird, Utah),* Proceedings of the International Topical Conference on Optical Effects in Amorphous Semiconductors, AIP Conf. Proc. No. 120, edited by P. C. Taylor and S. Bishop (AIP, New York, 1984).

[3]Z E. Smith, S. Aljishi, D. Slobodin, V. Chu, S. Wagner, P. M. Lenahan, R. R. Arya, and M. S. Bennett, Phys. Rev. Lett. **57**, 2450 (1986).

[4]See, for example, *Amorphous Silicon and Related Materials,* edited by H. Fritzsche (World Scientific, Singapore, 1989), Vol. A, Ch. 2.

[5]R. A. Street, J. Kakalios, C. C. Tsai, and T. M. Hayes, Phys. Rev. B **35**, 1316 (1987).

[6]D. Slobodin, S. Aljishi, R. Schwarz, and S. Wagner, in *Materials Issues in Applications of Amorphous Silicon Technology,* Vol. 49 of *Materials Research Society Symposium Proceedings,* edited by D. Adler, A. Madan, and M. J. Thompson (MRS, Pittsburgh, 1985), p. 153.

[7]D. L. Staebler and C. R. Wronski, Appl. Phys. Lett. **31**, 292 (1977).

[8]Z E. Smith, S. Aljishi, D. S. Shen, V. Chu, D. Slobodin, and S. Wagner, *Stability of Amorphous Silicon Alloy Materials and Devices,* Proceedings of an International Conference on Stability of Amorphous Silicon Alloy Materials and Devices, AIP Conf. Proc. No. 157, edited by B. L. Stafford and E. Sabisky (AIP, New York, 1987), p. 171.

[9]T. J. McMahon and R. Tsu, Appl. Phys. Lett. **51**, 412 (1987).

[10]X. Xu, A. Morimoto, M. Kumeda, and T. Shimizu, Appl. Phys. Lett. **52**, 622 (1988).

[11]For samples grown in our laboratory from dc glow discharges in SiF_4, GeF_4, and H_2-gas mixture, the Tauc gap E_g and the germanium concentration x_{Ge} follows an empirical relation $E_g = 1.73 - 0.91 x_{Ge}$ for $1.2 \leq E_g \leq 1.7$ eV (Ref. 6).

[12]S. Wagner, V. Chu, D. S. Shen, J. P. Conde, S. Aljishi, and Z E. Smith, in *Materials Issues in Amorphous-Semiconductors Technology,* Vol. 118 of *Materials Research Society Symposium Proceedings,* edited by Y. Hamakawa, P. G. LeComber, A. Madan, P. C. Taylor, and M. J. Thompson (MRS, Pittsburgh, 1988), p. 623.